PHYSICAL REVIEW B

CONDENSED MATTER

THIRD SERIES, VOLUME 27, NUMBER 8 15 APRIL 1983

Electron and positron response to atomic defects in solids: A theoretical study of the monovacancy and divacancy in aluminum

Bulbul Chakraborty* and R. W. Siegel

Materials Science and Technology Division, Argonne National Laboratory, Argonne, Illinois 60439

(Received 23 December 1982)

A formalism for self-consistently calculating the response of electrons and positrons to atomic defects in solids is presented. The formalism can be used with either the Green's-function or supercell method for calculating defect characteristics, and is of general applicability. With the use of this formalism and the self-consistent pseudopotential scheme within a supercell, the electronic structure and positron states and annihilation characteristics associated with the monovacancy and divacancy in aluminum have been studied. The sensitivity of the calculated monovacancy electronic structure and formation energy to the type of ionic pseudopotential used is also examined. Finally, the possibilities for using positron-annihilation spectroscopy to study the electronic structure of vacancylike defects are considered.

I. INTRODUCTION

The study of the electronic structure of atomic defects in solids, besides being interesting and challenging in its own right, is important to the establishment of a fundamental understanding of the defect-related characteristics of solids. A considerable amount of theoretical and experimental effort has, therefore, been expended in trying to understand the structure of defects, both qualitatively and quantitatively. Realistic electronic structure calculations of atomic defects have recently become possible because of the advent of the supercell[1-4] and the Green's-function[5-7] methods. Such calculations can yield detailed information about atomic defects, which in conjunction with experimental studies can provide valuable spectroscopic information about the nature of the defect state. In metals, few experimental techniques are available for detailed spectroscopy of defects, and only positron-annihilation spectroscopy (PAS) is generally applicable as a sensitive localized probe of vacancylike defect structures.[8,9] It is therefore desirable to complement PAS experimental studies with theoretically calculated positron-annihilation characteristics of specific defects, in order to allow for the possibility to obtain quantitative detailed information about the nature of such defect states in metals from PAS. In most other experimental techniques, a single number (e.g., the defect formation energy in an investigation of vacancy formation) is essentially all that becomes available for comparison with theory. This is an undesirable situation, first of all because of the dependence on a single number, and furthermore because it is extremely difficult to calculate such defect parameters as the formation energy from first principles with sufficient accuracy,[3,4] and the results may not necessarily be a sensitive measure of the nature of the defect in any event.

The positron-annihilation characteristics of a defect cannot be directly deduced from its calculated electronic structure in the absence of the positron, because the positron perturbs its electronic environment. Calculations of the electronic structure of defects, therefore, have to be complemented by separate calculations of their positron-annihilation characteristics, including electron-positron correlation effects, in order to be able to make complete use of the experimental information that can be made available regarding defects. A generalized self-consistency scheme for calculating positron-annihilation characteristics has been developed recently,[10] based on a two-component density-functional formalism; the scheme is of general applicability and can be incorporated into any electronic structure calculation method: for example, either the supercell or Green's-function method. In this paper the application of this formalism to atomic

defects is discussed.

Results of a supercell, self-consistent pseudopotential calculation of the electronic structure and positron-annihilation characteristics of a monovacancy and a divacancy in aluminum are presented in this work. A brief report of the electronic structure work has been presented previously.[4] In Sec. II, the electronic structure calculations are discussed, their applicability to other systems is also considered, and the results of these calculations on aluminum are presented. In Sec. III, the formalism for calculating positron-annihilation characteristics of defects, including electron-positron correlation effects, is presented. In Sec. IV, this formalism is applied to the two specific defects. The results are then analyzed in terms of being able to obtain detailed electronic structure information regarding defects from positron-annihilation experiments.

II. ELECTRONIC STRUCTURE

The environment of the vacancy defects in aluminum was simulated by a 27-atom-site face-centered-cubic supercell,[2] and a self-consistent pseudopotential scheme was applied to this superlattice in order to obtain the electronic structure.[3,4] The supercell approach was chosen here in preference to the Green's-function method, because, in a metal, true self-consistency is difficult to achieve with the Green's-function scheme.[11] The electronic structure of a monovacancy in aluminum had been calculated previously using an empirical ionic pseudopotential.[3] In the present work an *ab initio,* norm-conserving, ionic pseudopotential[4] has been used, since the *ab initio* pseudopotential is better suited for doing self-consistent calculations.[12] Comparison of the results of the two calculations yields valuable information about the sensitivity of the calculated properties to the potential.

A. Bulk properties

Before embarking on the defect electronic structure calculations with the *ab initio* potential, the bulk properties of aluminum were calculated using each of the potentials. The results of the calculations are compared in Table I. It is seen that the *ab initio* potential yields results in much better agreement with experimental observations than does the empirical potential. A plane-wave basis set, with ~ 50 plane waves per atom, was used for both calculations; an additional ~ 50 plane waves were included via the Löwdin perturbation scheme.[3] The total-energy calculation is described in detail in Ref. 3 and more briefly in Sec. II B. The Brillouin-zone sampling was done using 89 $\vec{k}$ points in the irreducible $\frac{1}{48}$th of the zone. The tolerance criterion used for the self-consistency scheme was 10^{-6} Ry. These conditions were essential for obtaining well-converged results for the bulk properties. It is expected that to obtain the same type of accuracy in total-energy calculations in the supercell, similar conditions would have to be maintained. This is, however, near impossible because of computing-time restrictions. For a 26-atom supercell ~ 1300 plane waves (i.e., 50 plane waves per atom) would be needed to expand the wave functions, which would imply diagonalizing a matrix of that order, a formidable task. This basis-function restriction is a major obstacle of the supercell method with regard to total-energy calculations. However, it is apparent that the electronic structure can be calculated accurately with less stringent requirements.

TABLE I. Calculated bulk properties of aluminum at 0 K compared to experiment (extrapolated to 0 K) and results of other theoretical calculations. In Ref. 13 an *ab initio* potential similar to the one used here was used, but more stringent convergence requirements were imposed.

	Lattice constant (Å)	Bulk modulus (10^{12} dyn cm^{-2})
Ab initio pseudopotential		
(i) Present calculation	4.047	0.99
(ii) Reference 13	4.010	0.715
Empirical pseudopotential		
Present work	3.870	1.20
Full potential		
Reference 14	4.015	0.80
Experiment		
Reference 15		
(a)	4.031	0.722
(b)	4.045	
(c)		0.88

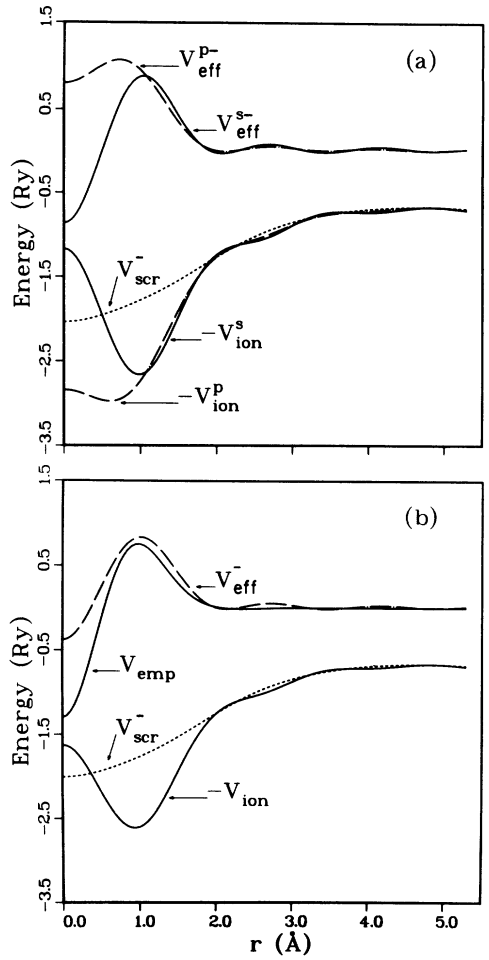

FIG. 1. Spherical averages of the components of the monovacancy potential V^{-}_{eff} experienced by the electrons. The screening potentials are denoted by V^{-}_{scr} and the Al ionic potentials by V_{ion}. The results of the *ab initio* nonlocal pseudopotential calculation (a), showing the *s* and *p* components separately, are compared to those of the empirical potential calculation (b). V_{emp} represents the empirical starting potential used in both of the calculations.

B. Monovacancy

The details of the defect electronic structure calculations are also described in Ref. 3. The same number of basis functions ($\sim$500 plane waves) were used here for the *ab initio* pseudopotential calculation as were used in the previous calculations, and the same convergence criteria were also retained. Furthermore, the identical empirical starting potential for the vacancy [V_{emp} in Fig. 1(b)] was used in each of the calculations. The resulting spherical averages of the monovacancy potentials, the difference in potential between the supercell containing a monovacancy and a defect-free supercell, for the empirical and *ab initio* potentials are shown in Fig. 1. The *ab initio* potential is nonlocal (i.e., angular momentum dependent). The screening parts of the two defect potentials are seen to be very similar. The essential difference between the two sets is the nonlocality. The local ionic potential is seen to be close to, although not exactly, an appropriately weighted average of the *s*- and *p*-ionic *ab initio* potentials. Some long-range oscillations are observed in Fig. 1, though the perturbing potentials are essentially short ranged. This long-range oscillatory behavior could lead to some defect-potential overlap in the supercell near the third-nearest neighbors (at $r=5.0$ Å). The overlap is not large enough to affect the resulting electronic structure significantly, but could introduce an appreciable error into the calculation of the formation energy. The electron density around the monovacancy, calculated using the *ab initio* potential, is shown in Fig. 2 and compared to results of the empirical-potential calculation.[3] The results for the electron density in the monovacancy are slightly different for the two potentials. The value of the electron density at the center of the monovacancy, 2.93×10^{-3} a.u. (the average electron density in Al is 2.68×10^{-2} a.u.), is higher for the *ab initio* potential than the empirical-potential result of 2.48×10^{-3} a.u. The other noticeable difference between the results of the two calculations is the variation in electron density from an atomic site to an interstitial site, which is smaller for the *ab initio* potential than for the empirical potential. The electron-density contours near an atom are also more spherical (atomlike) for the *ab initio* pseudopotential calculation. These differences do not seem to be appreciable in terms of the electronic structure but, as will be shown later, they lead to a significant difference ($\sim$0.4 eV) in the calculated vacancy-formation energy.

The reciprocal-space formulation of the total energy leads to the following expression[3] for the total energy E_{tot}:

$$E_{\text{tot}}=\sum_{k}^{\text{occ}}\epsilon_k-\tfrac{1}{2}\sum_{\vec{G}\neq0}^{\vec{G}^{(1)}_{\max}}V_{\text{Coul}}(\vec{G})n(\vec{G})-\sum_{\vec{G}}^{\vec{G}^{(1)}_{\max}}V_{\text{xc}}(\vec{G})n(\vec{G})+\sum_{\vec{G}}^{\vec{G}^{(1)}_{\max}}\epsilon_{xc}(\vec{G})n(\vec{G})+\alpha Z+E_{\text{Ewald}}\ . \quad (1)$$

Here, the ϵ_k are the calculated eigenvalues, $V_{\text{Coul}}(\vec{G})$ are the $\vec{G}$ components of the Coulomb term, $V_{\text{xc}}(\vec{G})$ are the components of the exchange-correlation potential, the $\epsilon_{\text{xc}}(\vec{G})$ are the components of the exchange-correlation energy, and $n(\vec{G})$ is the elec-

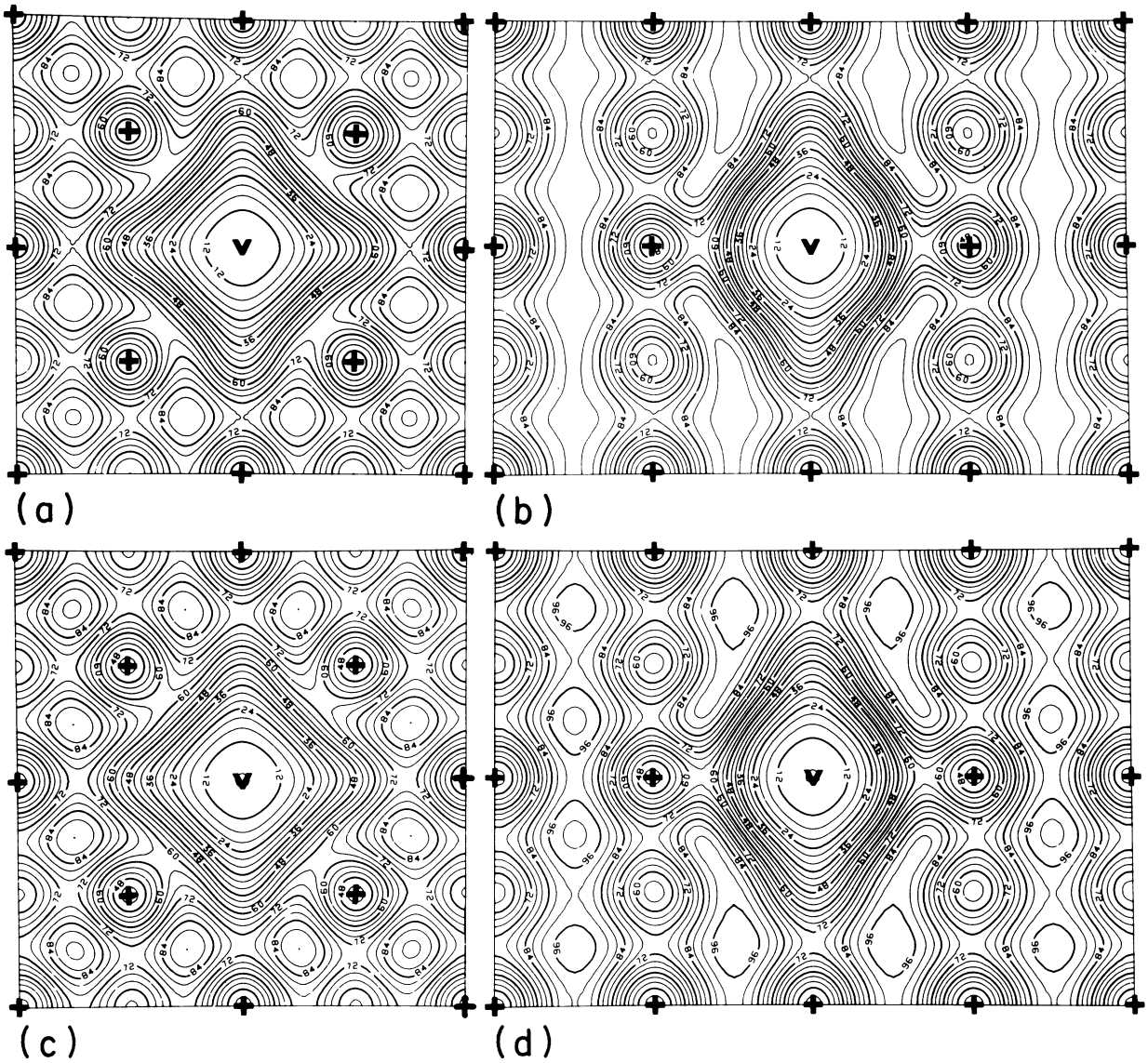

FIG. 2. Valence-electron pseudodensity (times the supercell volume) around a vacancy (V) in [(a),(c)] the (100) plane and [(b),(d)] the (110) plane of the supercell. Results for the *ab initio* pseudopotential calculation [(a),(b)] are compared to those obtained from the empirical potential calculation [(c),(d)] in Ref. 3. The atomic positions are denoted by $+$.

tron pseudodensity. The term αZ is a correction due to the pseudonature of the potential,[3] which measures its repulsiveness, and E_{Ewald} is the Ewald core-core interaction energy.[16] The determination of the summation limit $\vec{G}^{(1)}_{\text{max}}$ is described in Ref. 3; about 1600 $\vec{G}$ components were included in the summation for the vacancy. The calculated values for the various components of the total energy for the two potentials are compared in Table II. The value for the monovacancy formation energy calculated with the *ab initio* potential, 1.5 eV, is seen to be smaller than that calculated previously with the empirical potential,[3] 1.9 eV, but, nevertheless, still too large compared to the experimental value of 0.66 eV.[17,18] There could be two major reasons for this discrepancy between theory and experiment: (i) lattice relaxation effects and (ii) difficulties associated with the supercell method.

Atomic relaxations can, in principle, be calculated in the self-consistent pseudopotential scheme by calculating the forces on the nearest-neighbor atoms by the Hellmann-Feynman method and then minimizing these forces.[3] For the empirical potential, the first-neighbor relaxations around the monovacancy were calculated to be $\sim 2\%$ radially inward displacements, a relatively small effect. The relaxation energy would, therefore, not be expected to be large enough to account for the difference between theory

TABLE II. Components of the total energy per atom of a 27-atom-site supercell with and without a vacancy. The results from the present *ab initio* calculation are compared to the previous empirical potential results (Ref. 3). The formation energy is obtained by taking the difference in total energy per atom and multiplying by 26. The prime on the summation indicates that the $\vec{G}=0$ term is excluded.

	Ab initio pseudopotential ($a=4.047$ Å)		Empirical pseudopotential[a] ($a=4.045$ Å)	
Total-energy components	Vacancy (Ry)	Bulk	Vacancy (Ry)	Bulk
$\sum_k \epsilon_k$	−0.6890	−0.6665	−0.6269	−0.6026
$\frac{1}{2}\sum' V_{\text{Coul}}(\vec{G})n(\vec{G})$	0.0576	0.0051	0.0582	0.0070
$\sum[\epsilon_{\text{xc}}(\vec{G})-V_{\text{xc}}(\vec{G})]n(\vec{G})$	0.4851	0.4829	0.4851	0.4829
αZ	1.3515	1.3515	1.2755	1.2755
E_{Ewald}	−5.3169	−5.3938	−5.3109	−5.3898
E_{tot}	−4.2269	−4.2311	−4.2355	−4.2409
E_{1v}^{F}	0.11(1.5eV)		0.14(1.9eV)	

[a]Reference 3.

and experiment. However, there is a significant uncertainty present in the calculated relaxation parameters. The cumulative supercell effects would appear to be the dominant source of errors. One of these is the effect of spurious vacancy-vacancy overlaps introduced by the supercell. Such overlaps could, in principle, be reduced by increasing the size of the supercell. However, this would require a basis set which is too large to be handled within reasonable computational resources. The larger the supercell, therefore, the more drastic is the effect of the basis-set restriction, since the number of basis functions per atom has to be reduced to stay within reasonable computational costs. Even with the present 27-atom-site supercell, basis-set inadequacies appear to have negatively affected the resulting vacancy-formation energy (cf. Sec. II A). This problem could be solved partially by using a mixed basis set,[19] but this is not expected to improve the situation for a metal like aluminum. Even for transition metals, and using a mixed basis set, the basis set needed for an adequate formation-energy calculation is expected to be too large to be handled numerically. We seem to be arriving at the conclusion, therefore, that the supercell method is not suitable for accurate formation-energy calculations within present computational limitations. Similar computational limitations, but with regard to self-consistency difficulties and not overlap, are also present in the Green's-function method. Formation-energy calculations are thus probably more efficiently approached from a density-matrix-type method,[20] which does not yield detailed spectroscopic information, but which is apparently well suited for energetic calculations.

C. Divacancy

The self-consistent pseudopotential supercell method, with either a plane-wave or a mixed basis set is, nevertheless, extremely useful for obtaining detailed information about the local electronic structure of defects, the type of information that may be obtained from positron-annihilation spectroscopy experiments. With this view in mind, the *ab initio* pseudopotential method was further applied to the calculation of the electronic structure of a divacancy in aluminum, and then also to calculations of the positron-annihilation characteristics of the monovacancy and divacancy in aluminum. The environment of the divacancy was again simulated by a 27-atom-site supercell, with the divacancies oriented along one of the ⟨110⟩ directions. In this configuration, nearest-neighbor divacancies share some common first-nearest-neighbor atoms. The overlap between divacancies is, therefore, expected to be of greater consequence in the electronic structure calculation than was the monovacancy-monovacancy overlap. However, for the purpose of calculating the positron-annihilation spectra, the errors introduced by these overlaps are expected to be small, since the positron localization in these deeper traps is rather strong. These errors become only really significant in the context of formation-energy calculations, which were shunned for this case. The convergence requirements imposed on the divacancy calculations were much less stringent than those used for the monovacancy formation energy and electronic structure calculations. The basis set included ~300 plane waves here, compared to ~500 plane waves for the monovacancy, which allowed the eigenvalues

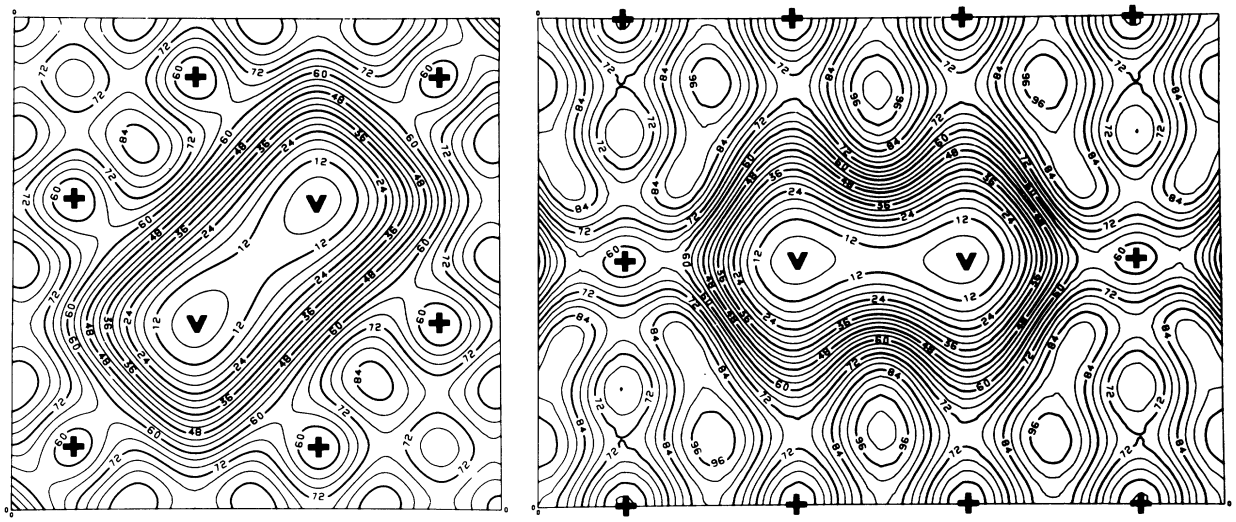

FIG. 3. Valence-electron pseudodensity (times the supercell volume) around a divacancy (V-V) in (a) a (100) plane and (b) a (110) plane of the supercell containing the divacancy. The atomic positions are denoted by $+$.

to be converged to 10^{-2} Ry (compared to 10^{-3} Ry in the monovacancy case). The tolerance criterion for self-consistency was at least 10^{-3} Ry ($\sim$0.01 eV) for all components of the screening potential. The 10 special-$\vec{k}$-point scheme[3] was used for sampling the Brillouin zone. The number of Fourier components included in the charge-density calculation was $\sim$1000.

The calculated electron density around the divacancy is shown in Fig. 3 for the (100) and (110) planes containing the two vacancies. It can be clearly seen that there is significant perturbation of the electronic structure in the vicinity of the common nearest-neighbor atom sites, along the major axis of the divacancy. But again, this is important only in the context of formation-energy calculations, and can be essentially neglected for positron-annihilation studies, since, as will be seen later, the positron is very well localized within a divacancy. The value of the electron density at the center of either of the vacancies forming the divacancy is considerably lower, 2.2×10^{-3} a.u., than the value at the center of a monovacancy (2.93×10^{-3} a.u.). The electron density at the center of mass of the divacancy is, however, considerably higher, 3.76×10^{-3} a.u. A plot of the difference in valence-electron density between a supercell containing no defects and one containing a divacancy is shown in Fig. 4 for a (100) plane containing the divacancy. It is seen that the perturbation is predominantly short ranged, and that the overlap of the electrons with the positrons can be expected to go to zero quite rapidly away from the divacancy. This will be demonstrated later on in the paper. It should be noted that this difference plot does not represent the actual situation very precisely, because the perfect-lattice electron density was calculated with convergence criteria identical to those for the monovacancy calculation, but quite different from those for the divacancy calculation. This can introduce quite a bit of noise in the difference spectrum, as seen in Fig. 4. The rest of the paper is devoted to the formalism and results of the positron-annihilation studies.

III. POSITRON ANNIHILATION: THEORETICAL FORMALISM

Calculations of the positron-annihilation characteristics of defects in real solids have previously suffered from the inability to include electron-positron correlation effects properly, although the correlation effects have been studied carefully in jellium models.[21] A formalism for carrying out realistic calculations of the positron-annihilation characteristics of defects is presented in this section. The salient features of such a calculation are (i) accurate treatment of the host electronic structure, (ii) self-consistent determination of the electron and positron densities and potentials, allowing for electronic screening of both the defect and the positron, and (iii) inclusion of the structural relaxations around the defect in the presence of the trapped positron. The first requirement is satisfied by both the supercell and the Green's-function methods. For the second condition to be satisfied, a generalization of the self-consistency scheme used in electronic structure calculations is needed. Such a scheme, obtained from a generalized density-functional approach, has been developed recently and applied to defect-free

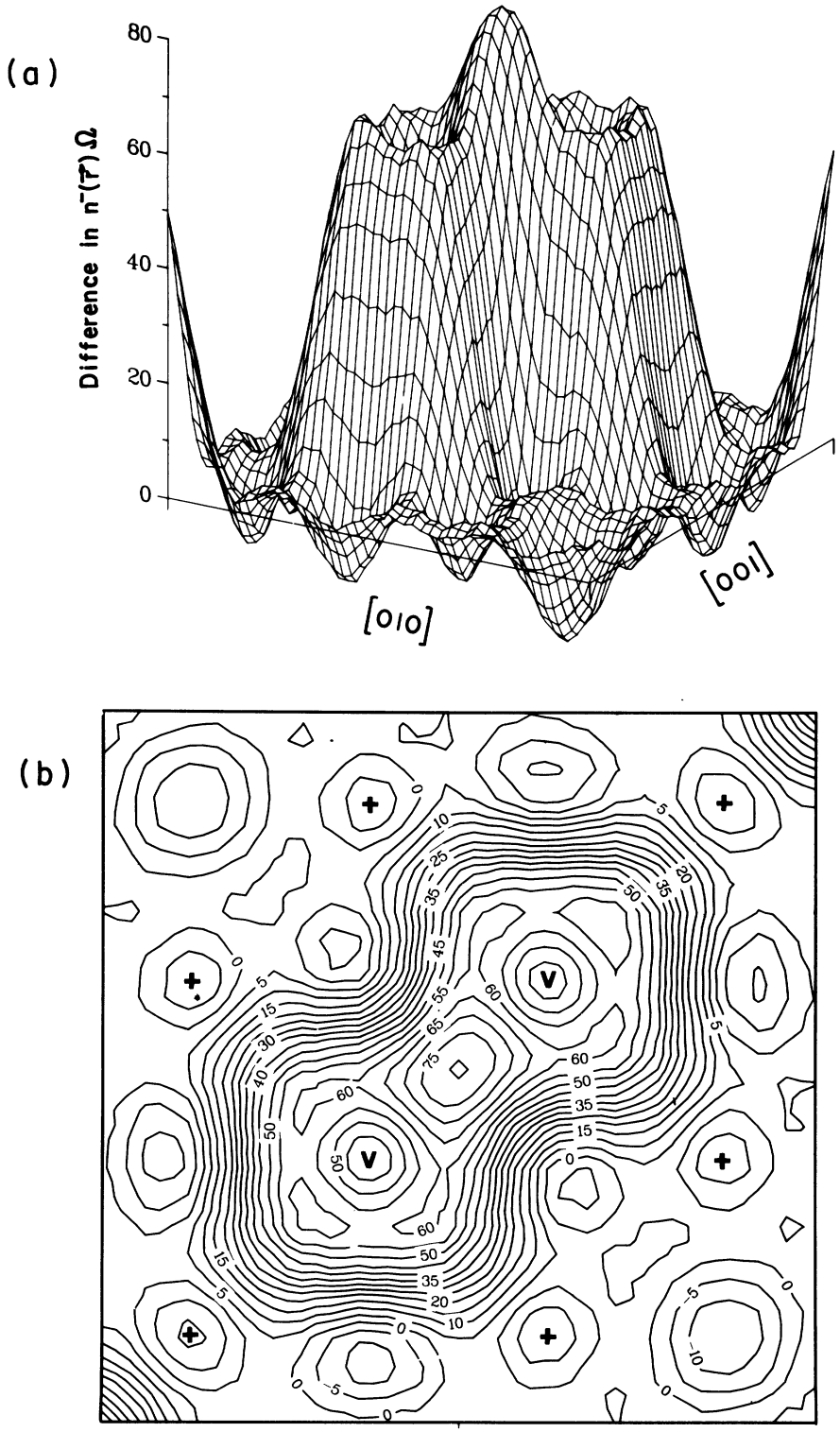

FIG. 4. Difference in valence-electron pseudodensity $n^-(\vec{r})$ (times the supercell volume Ω) between a supercell without and with a divacancy, shown in the (100) plane of the supercell, in (a) perspective and (b) contour representations. The addition of the core-electron densities would make this difference monotonic in the peak region, as would be expected.

aluminum.[10] In this section a description of the scheme as applied to defect studies using the supercell method is presented. Structural relaxations can also be treated within this scheme, in principle, but at present the numerical accuracies of such estimates attainable within reasonable computational times (costs) are insufficiently reliable to give quantitative information about the relaxed structure. Some qualitative information, however, can be obtained from calculating Hellmann-Feynman forces.[3] These results will be discussed for the case of the monovacancy in aluminum.

A. Self-consistency scheme

The derivation of the self-consistency scheme has been described briefly in Ref. 10. A detailed derivation, analogous to the spin-density-functional theory derivation[22] is presented in the Appendix. After making the necessary approximation for a single positron being present in the system (cf. Ref. 10 and the Appendix), the self-consistency equations can be written as

$$
\begin{aligned}
&\left[-\frac{\nabla^2}{2}+V_{\rm eff}^{-}(\vec{r})\right]\psi_i^{-}(\vec{r})=\epsilon_i^{-}\psi_i^{-}(\vec{r})\ ,\\
&\left[-\frac{\nabla^2}{2}+V_{\rm eff}^{+}(\vec{r})\right]\psi^{+}(\vec{r})=\epsilon^{+}\psi^{+}(\vec{r})\ ,\\
&V_{\rm eff}^{-}(\vec{r})=V^{-}(\vec{r})+V_{\rm Coul}(\vec{r})\\
&\qquad\qquad +\mu_{\rm xc}(n^{-}(\vec{r}),n^{+}(\vec{r}))\ ,\\
&V_{\rm eff}^{+}(\vec{r})=V^{+}(\vec{r})-V_{\rm Coul}(\vec{r})+\epsilon_{\rm corr}^{-+}(n^{-}(\vec{r}))\ ,\\
&\mu_{\rm xc}(\rho,\rho')=\rho\,\partial\epsilon_{xc}^{-}(\rho)/\partial\rho+\epsilon_{\rm xc}^{-}(\rho)\\
&\qquad\qquad +\rho'\,\partial\epsilon_{\rm corr}^{-+}(\rho)/\partial\rho\ ,\\
&n^{-}(\vec{r})=\sum_i|\psi_i^{-}(\vec{r})|^2\ ,\\
&n^{+}(\vec{r})=|\psi^{+}(\vec{r})|^2\ .
\end{aligned}
\tag{2}
$$

Here, $V^{-}(\vec{r})$ $[V^{+}(\vec{r})]$ are the external potentials (in a solid, the superposition of the ionic potentials) felt by the electron (positron), $V_{\rm Coul}(\vec{r})$ is the electrostatic potential due to the electrons, $\epsilon_{\rm corr}^{-+}(n^{-}(\vec{r}))$ is the electron-positron correlation energy of a homogeneous electron gas of density $n^{-}(\vec{r})$, and $\mu_{\rm xc}(n^{-}(\vec{r}),n^{+}(\vec{r}))$ is the combined exchange-correlation potential felt by the electrons. The set of equations given in Eq. (2) constitute the self-consistency scheme. It can be used to determine the electron and positron densities in any system, with a given geometry and external potentials.

In the supercell approach to the defect problem, periodicity is retained and the solutions of Eq. (2) are Bloch waves; hence solving Eq. (2) reduces to a band-structure problem with two eigenvalue problems to be solved at each self-consistency step. The positron external potential $V^{+}(\vec{r})$ is normally the negative of the electron external potential $V^{-}(\vec{r})$, which is given by

$$
V^{-}(\vec{r})=\sum_i V_{{\rm ion},i}(\vec{r}-\vec{R}_i)\ , \tag{3}
$$

where $V_{{\rm ion},i}(\vec{r}-\vec{R}_i)$ is the ionic potential at $\vec{r}$ from the ion at the site $\vec{R}_i$ of the superlattice. For a monovacancy, the ionic potential at one of the 27 supercell sites is zero. In the present work, the ionic potentials are replaced by *ab initio* pseudopotentials for the electrons, and a Kubica-Stott[23]—type pseudopotential for the positron. In this case, $V^{+}(\vec{r})$ is no longer simply the negative of $V^{-}(\vec{r})$. The positron pseudopotential scheme will be described in Sec. IV.

In the Green's-function scheme, Eq. (2) would first have to be solved for the perfect lattice to obtain both an electron and a positron Green's function.[6] The electron and positron states in the presence of a defect could then be expressed in terms of these Green's functions and the defect potentials $U^{-}(\vec{r})$ $[U^{+}(\vec{r})]$ for the electron (positron).[6] The defect potentials are defined as the differences between $V_{\rm eff}^{-}(\vec{r})$ and $V_{\rm eff}^{+}(\vec{r})$ for a solid with a defect and those for the perfect lattice. These potentials, therefore, have the same form as the $V_{\rm eff}(\vec{r})$ of Eq. (2) and can be determined self-consistently. At each iteration step, $U^{-}(\vec{r})$ and $U^{+}(\vec{r})$ are recalculated from the values of $n^{-}(\vec{r})$ and $n^{+}(\vec{r})$ obtained from the previous iteration. The difference here from a purely electronic calculation is the necessity to determine two sets of densities and potentials at each self-consistency step.

B. Angular correlation spectra and positron lifetimes

In positron-annihilation experiments, information regarding the electron momenta and density overlapped by the positron can be obtained through measurements of the angular correlation of the positron-electron annihilation γ rays and positron lifetime, respectively. To calculate these quantities, the electron-positron pair momentum distribution $R(\vec{p})$ has to be calculated. The expression for $R(\vec{p})$ is

$$
\begin{aligned}
R(\vec{p})=&\int d\vec{r}\,d\vec{r}\,'\exp[i\vec{p}\cdot(\vec{r}-\vec{r}\,')]\\
&\times\langle\Phi^{+\dagger}(\vec{r})\Phi^{+}(\vec{r}\,')\Phi^{-\dagger}(\vec{r})\Phi^{-}(\vec{r}\,')\rangle\ .
\end{aligned}
\tag{4}
$$

Here, Φ^{+} and Φ^{-} are the positron and electron field operators, respectively, and the angular brackets denote the ground-state expectation value. Express-

ing the field operators in terms of the wave functions ψ_i^- and ψ^+ of Eq. (2) and the creation (destruction) operators $c_i^\dagger$ (c_i) and $d_0^\dagger$ (d_0) for ψ_i^- and ψ^+, respectively, Eq. (4) can be written as

$$R(\vec{p})=\sum_{i,j}\langle d_0^\dagger d_0 c_i^\dagger c_j\rangle \times\left[\int d\vec{r}\,d\vec{r}\,'\exp[i\vec{p}\cdot(\vec{r}-\vec{r}\,')]\times\psi^{+*}(\vec{r})\psi^+(\vec{r}\,')\psi_i^{-*}(\vec{r})\psi_j^-(\vec{r}\,')\right]. \tag{5}$$

In order to determine $R(\vec{p})$, the ground-state average $\langle d_0^\dagger d_0 c_i^\dagger c_j\rangle$ has to be calculated. The procedure for evaluating this function within the local-density approximation in an inhomogeneous system is given in the Appendix. The resulting expression for $R(\vec{p})$ is

$$R(\vec{p})=\sum_i N(\epsilon_i)\left|\int d\vec{r}\,e^{-i\vec{p}\cdot\vec{r}}\psi^+(\vec{r})\psi_i^-(\vec{r})\right|^2,$$
$$N(\epsilon)=\int d\vec{r}\,N^0(\epsilon,n^-(\vec{r}))n^+(\vec{r}). \tag{6}$$

In this equation, $N^0(\epsilon,n^-(\vec{r}))$ is the electron-positron pair momentum distribution function in a homogeneous electron gas of density $n^-(\vec{r})$, expressed as a function of the energy $\epsilon=p^2/2m$. The function $N^0(\epsilon,n^-(\vec{r}))$ is known from many-body calculations in an electron gas.[24,25] Thus the momentum distribution and, hence the angular correlation spectra can be calculated from a knowledge of the energies and wave functions calculated using Eq. (2). The reciprocal of the positron lifetime $\tau^{-1}\equiv\Lambda$ is an integral of $R(\vec{p})$ over all $\vec{p}$ and can be determined from

$$\Lambda=\int d\vec{r}\,n^+(\vec{r})\lambda(\vec{r}),$$
$$\lambda(\vec{r})=\sum_i N(\epsilon_i)\,|\psi_i^-(\vec{r})|^2. \tag{7}$$

If $N(\epsilon)$ is replaced by the Fermi distribution function, $\lambda(\vec{r})$ reduces to $n^-(\vec{r})$, and we recover the independent-particle model result for the lifetime. In a Brandt-Reinheimer formulation for calculating the electron-density enhancement,[21] $\lambda(\vec{r})$ is replaced by $\lambda^0(n^-(\vec{r}))$, the positron lifetime in a homogeneous electron gas of density $n^-(\vec{r})$.

C. Core contribution

The preceding discussion of the formalism for calculating positron-annihilation characteristics was tacitly restricted to a consideration of the valence electrons. The contribution from core electrons, especially for positrons trapped in defects, is a small, but non-negligible, fraction of the valence-electron contribution. The momentum distribution from core electrons, $R^{\rm core}(\vec{p})$, can also be calculated from Eq. (6); however, with $\psi_i^-(\vec{r})$ replaced by $\psi_i^{\rm core}(\vec{r})$, a core-electron wave function, the function $N(\epsilon_i)$ replaced by $N_i^{\rm core}$, the enhancement for a particular core state, and the summation running over all core states. In analogy to the derivation of $N(\epsilon)$, $N^{\rm core}$ can be written as

$$N^{\rm core}=\int d\vec{r}\,n^+(\vec{r})N^0(p,\rho(\vec{r})). \tag{8}$$

Here, p is the momentum of a core state and $\rho(\vec{r})$ is the core-electron density. Other formulations for calculating the core enhancement exist in the literature.[26] The one presented here is the one most closely analogous to the valence formulation. A different approximation might be obtained by replacing $N^0(p,\rho(\vec{r}))$ by an average enhancement factor $\langle N^0(\rho(\vec{r}))\rangle_{\rm av}$ for $p\le p_F$, the Fermi momentum, and zero otherwise, as suggested in Ref. 26. It has been shown that the two approximations yield significantly different results for defect-free aluminum,[10] but the net resulting uncertainties for defect applications are small. The core-electron contribution to the positron lifetime can be obtained in a manner analogous to the calculation of the valence-electron contribution. In the next section we describe the results of the application of the theoretical method described here to calculating the positron-annihilation characteristics of monovacancies and divacancies in aluminum.

IV. POSITRON ANNIHILATION FROM VACANCIES IN Al

To calculate the positron-annihilation characteristics, a supercell identical to that used in the vacancy defect electronic structure calculations was employed and the same *ab initio* norm-conserving ionic pseudopotential was used for $V^-(\vec{r})$ in Eq. (2). The positron pseudopotential method of Kubica and Stott[23] was utilized to replace $V^+(\vec{r})$ by a pseudopotential. In this method the positron wave function $\psi^+(\vec{r})$ is written as a product of a pseudo-wavefunction $\phi^+(\vec{r})$ and a Wigner-Seitz (WS) type of function $U^+(\vec{r})$; thus $\psi^+(\vec{r})=\phi^+(\vec{r})U^+(\vec{r})$, where $U^+(\vec{r})$ satisfies the boundary conditions

$$U^+(\vec{r})=U_0^+(\vec{r}),\quad |\vec{r}|<R_{\rm WS}$$
$$U^+(\vec{r})=U_0^+(R_{\rm WS}),\quad |\vec{r}|\ge R_{\rm WS}$$
$$\left[\frac{dU^+(\vec{r})}{dr}\right]_{r=R_{\rm WS}}=0.$$

Here, $R_{\rm WS}$ is the radius of a sphere inscribed in the Wigner-Seitz cell. The solution $U_0^+(\vec{r})$ satisfies the

following Schrödinger equation:

$$\left[-\frac{\nabla^2}{2}+V_{\rm WS}(\vec{r})\right]U_0^+(|\vec{r}|)=E_0U_0^+(|\vec{r}|)\,, \tag{9}$$

where $V_{\rm WS}(\vec{r})$ must be similar to the actual potential within $R_{\rm WS}$, but is arbitrary otherwise. The equation for the pseudo-wave-function is [cf. Eq. (2)],

$$\left[-\frac{\nabla^2}{2}+V^+_{\rm pseudo}(\vec{r})-V_{\rm Coul}(\vec{r})+\epsilon^{-+}_{\rm corr}(n^-(\vec{r}))\right]\phi^+(\vec{r})=\epsilon^+\phi^+(\vec{r})\,, \tag{10}$$

$$V^+_{\rm pseudo}(\vec{r})=V^+(\vec{r})-V_{\rm WS}(\vec{r})+E_0-\left[\frac{d}{dr}\ln U_0^+(\vec{r})\right]\hat{r}\cdot\vec{\nabla}\,,$$

where $V^+_{\rm pseudo}(\vec{r})$ is the ionic pseudopotential for the positron. In our calculations the gradient term in Eq. (10) was neglected, which eliminated the wave-function dependence of the pseudopotential. Therefore, a convenient form of $V^+_{\rm pseudo}(\vec{r})$ could be chosen for the self-consistent calculations, and $V_{\rm WS}(\vec{r})$ then obtained from Eq. (10). Since the term E_0 causes only a shift of the energy zero, this procedure is possible. The procedure used here is different from that employed in Ref. 24, in which a form for $V_{\rm WS}(\vec{r})$ was chosen first and then Eq. (10) was used to determine $V^+_{\rm pseudo}(\vec{r})$. In the present work, the ionic potential for aluminum was first calculated using a self-consistent Dirac-Slater scheme. This potential was then fitted to an Appelbaum-Hamann[27] form of pseudopotential, such that the pseudopotential $V^+_{\rm pseudo}(\vec{r})$ was matched smoothly to the ionic potential at the inscribed sphere radius. The pseudo-wave-function was determined self-consistently and $U_0^+(|\vec{r}|)$ was calculated once using Eq. (9). In the following we will denote the positron pseudodensity by $n^+(\vec{r})\equiv|\phi^+(\vec{r})|^2$, and the actual density by $\rho^+(\vec{r})\equiv|\psi^+(\vec{r})|^2$.

A. Positron properties in vacancies

The present calculations were carried out for the 0-K lattice constant of aluminum, 4.0469 Å, and for two other larger lattice constants. Here, we will primarily discuss the 0-K results, and bring in the results from the other calculations only for comparison purposes. The results for the larger lattice constants, representative of higher temperatures, are being presented elsewhere.[28] Preliminary reports of some of the 0-K results have appeared previously.[29]

The effective potential $V^+_{\rm eff}(\vec{r})$, experienced by the positron, and its various components centered at a monovacancy and a divacancy are shown in Fig. 5. The spherical averages are shown to give a general idea of the depth and extent of the trapping potentials. As is to be expected, there is considerable anisotropy of the trapping potentials, especially for the divacancy; these anisotropies are evident from the calculated distributions of the defect-trapped positrons (Fig. 6). Bound states of the positron exist for both the monovacancy and divacancy. The calculated positron binding energies for the two defects are shown as a function of lattice constant in Table III,

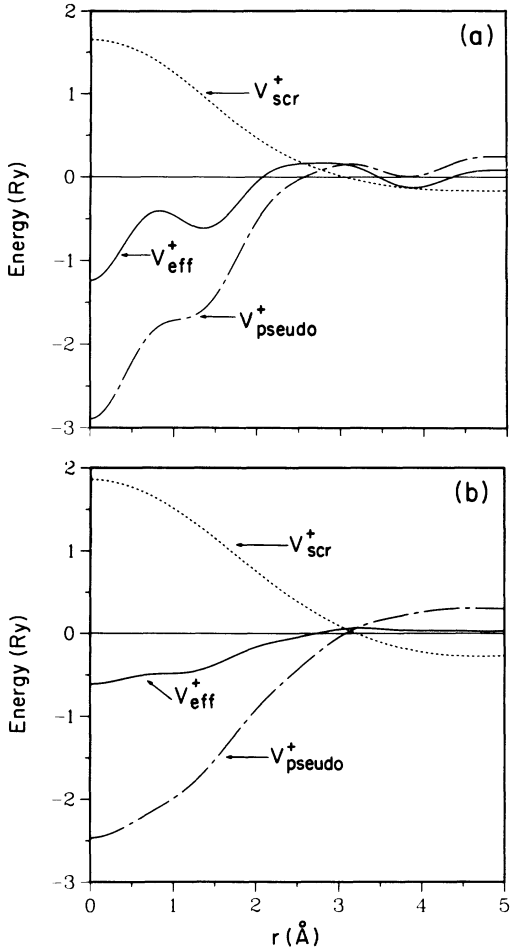

FIG. 5. Components of the effective potential $V^+_{\rm eff}$ experienced by the positron in the presence of (a) a monovacancy and (b) a divacancy. The screening potential is denoted by $V^+_{\rm scr}$ and the ionic pseudopotential by $V^+_{\rm pseudo}$. In order to give some idea about the average depth and range of the trapping potentials, spherical averages are presented; the magnitudes beyond the limits of the defects are, therefore, not indicative of those at any particular lattice or interstitial site. The centers of mass of the monovacancy and divacancy are at the origins.

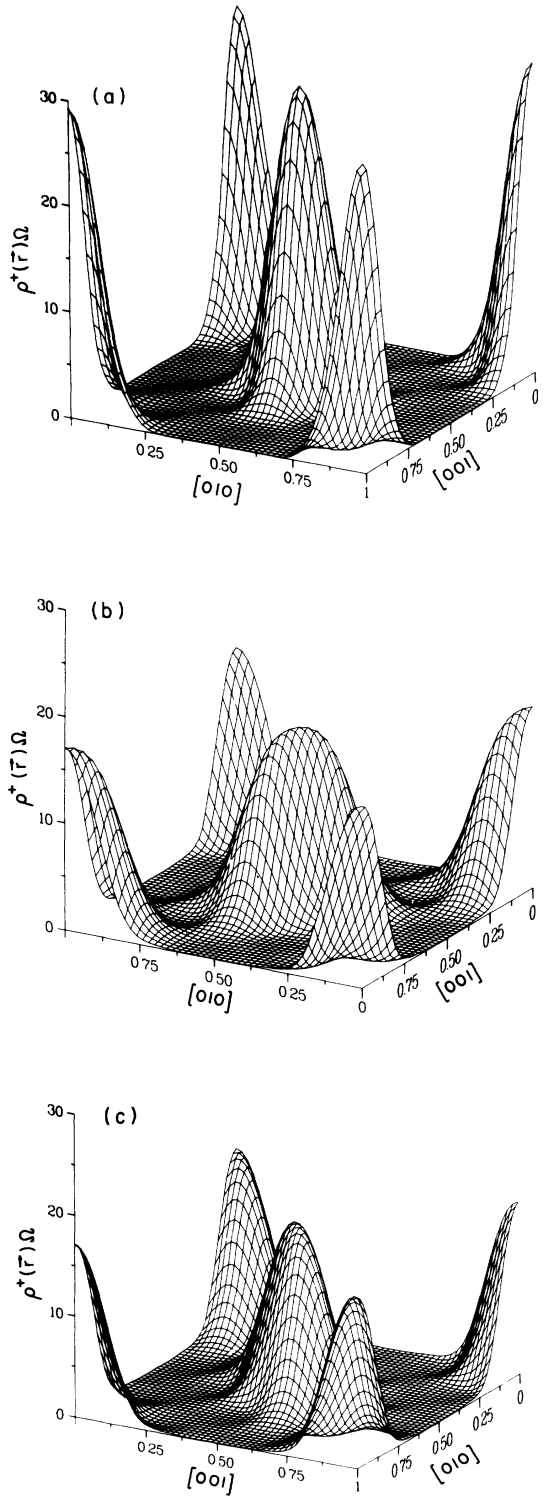

FIG. 6. Positron density $\rho^+(\vec{r})$ (times the supercell volume Ω) in the (100) plane around (a) a monovacancy (V) and [(b),(c)] a divacancy (V-V), shown in perspective. Two perspectives of $\rho^+(\vec{r})\Omega$ for the divacancy are shown to clarify the full asymmetries involved.

and compared to the results of other theoretical calculations. The only previous band-structure calculation of the binding energy of a positron in a monovacancy was a non-self-consistent augmented-plane-wave (APW) calculation in a supercell.[2] The work of Nieminen and Puska[30] emphasized solving for the positron wave function accurately for a given positron potential; the electron density was obtained from superposition of atomic charge densities, but no electronic rearrangement was taken into account. The other results[31] shown in Table III were based on a jellium model. These are taken as representative, although a number of additional such calculations exist.[21] The binding energies are seen to be rather sensitive to the calculation scheme.

The calculated positron densities $\rho^+(\vec{r})$ in the vacancy defects are shown in Fig. 6 as perspective representations on the (100) plane. The positron is seen to be extremely well localized in both the monovacancy and divacancy. Since the positron exists in bound states in these defects, it is interesting to look at the positron density of states. The positron densities of states in the presence of a monovacancy have been calculated and are shown in Fig. 7. The signature of a bound state is a sharp peak whose intensity diminishes on going away from the vacant site, a behavior shown by the local densities of states well below the bottom of the band. The densities of states were calculated using the tetrahedron scheme,[32] but using only four tetrahedra in the Brillouin zone. This introduces considerable noise into the spectrum, even though the Brillouin zone is 27× smaller for the supercell than for the one-atom cell; this noise was reduced by means of a smoothing function in Fig. 7. The bound-state characteristic is, however, little affected by this approximation, because there is hardly any dispersion of this state. There is a feature at about 0.15 Ry that looks like a resonance, but this could be an artifact of the calculation. In contrast to the positron density of states, the electron density of states in the absence of the positron did not show any signs of a bound electron state.[3] In the present work, furthermore, the electron density of states was seen to be quite insensitive to the presence of the positron. At present, there are no experimental observations of the positron density of states in the presence of defects. However, the positron experiments probing surfaces could benefit from a knowledge of the calculated local positron density of states near a surface.

B. Annihilation characteristics

For the calculations in aluminum, the functions $\epsilon_{\rm corr}^{-+}(n^-(\vec{r}))$ and $N^0(\epsilon, n^-(\vec{r}))$ were obtained from Ref. 24. Since periodicity is retained in a supercell, the calculation of $R(\vec{p})$ is conveniently carried out

TABLE III. The calculated positron binding energies to a monovacancy and a divacancy compared to results of other theoretical calculations. The lattice constant a used in each of the calculations is specified.

	Binding energy (eV)	
	Monovacancy	Divacancy
Present calculation		
(i) $a=4.0469$ Å	2.17	2.98
(ii) $a=4.1200$ Å	2.05	
(iii) $a=4.1323$ Å		2.85
Nieminen and Puska (Ref. 30) ($a=4.0469$ Å)	2.31	3.30
McMullen *et al.* (Ref. 31) ($a=4.0412$ Å)	1.56	3.19[a] 2.60[b]
APW calculation (Ref. 2) ($a=4.0483$ Å)	3.36	

[a]Spherical divacancy.
[b]Elliptical divacancy.

in reciprocal space, and

$$R(\vec{p})=\sum_{\vec{k},n,\vec{G}} N(\epsilon_{\vec{k}n})\,|A_{\vec{k}n}(\vec{G})|^2\,\delta(\vec{p}-\vec{k}-\vec{G})\,, \tag{11}$$

$$A_{\vec{k}n}(\vec{G})=\int d\vec{r}\exp[-i(\vec{k}+\vec{G})\cdot\vec{r}] \times\psi^{-}_{\vec{k}n}(\vec{r})\psi^{+}(\vec{r})\,,$$

where $\vec{G}$ are the reciprocal-lattice vectors, and $\vec{k}n$ denotes a Bloch state of wave vector $\vec{k}$ and band index n. Since the Brillouin zone is small in a supercell, a large number of $\vec{G}$ vectors are needed to determine $R(\vec{p})$ accurately. Because of computer limitations we could use only ~ 500 $\vec{G}$ vectors in the summation, which could have given rise to some noise in $R(\vec{p})$.

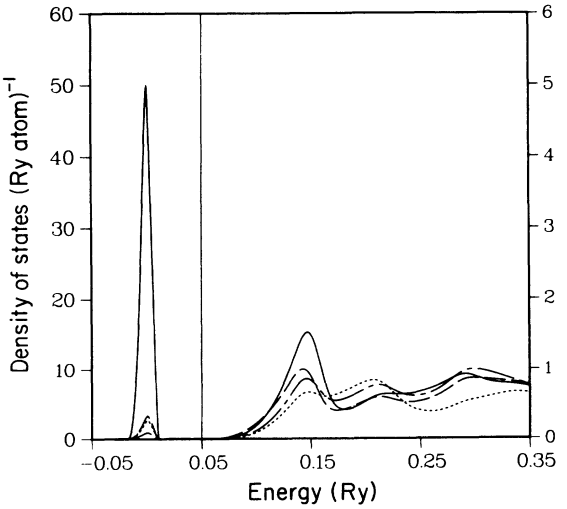

FIG. 7. Total (——) and local positron density of states in the presence of a monovacancy. The local density of states at the vacancy site (—), and the first- (---) and second- (—··—) nearest-neighbor sites are shown. The curves have been magnified by a factor of 10 in the energy region above 0.05 Ry, as indicated by the vertical line and right-hand scale. The band edge is at 0.16 Ry.

It is clear from the electronic structure information inherent in $R(\vec{p})$ that positron-annihilation experiments are capable of yielding detailed information regarding the electronic structure of defects in which positrons can be trapped. However, since the trapped positron probes only that region which it overlaps, and invariably perturbs, self-consistent theoretical calculations of the positron-electron overlap and the resulting positron-annihilation characteristics are necessary to facilitate the retrieval of the defect-specific information available from positron lifetime and momentum (e.g., angular correlation) experiments. Positron-lifetime measurements yield only rather integral information regarding the average electron density sampled by the positron in this overlap region. Although the positron lifetime is not very sensitive to the structure of the overlap, angular correlation spectra are much more sensitive to the details of the positron-electron overlap, and therefore inherently contain more defect-specific details. In Fig. 8, the overlap of $\lambda(\vec{r})$ and $\rho^{+}(\vec{r})$, the integral over which determines Λ [cf. Eq. (7)], is shown on the (100) plane for both the monovacancy and divacancy. On comparing these to the positron-density plots of Fig. 6, it is seen that the overlap shows more structure within the defects. The range of the overlap is predominantly determined by the range of the positron density. In the independent-particle model, the lifetime would be given by an integral over all space of the overlap between $n^{-}(\vec{r})$ and $\rho^{+}(\vec{r})$. This overlap shows essentially the same structure as $\lambda(\vec{r})\rho^{+}(\vec{r})$ even though the magnitude is not the same. In contrast, the overlap of $\lambda^{0}(n^{-}(\vec{r}))$ and $\rho^{+}(\vec{r})$, which determines

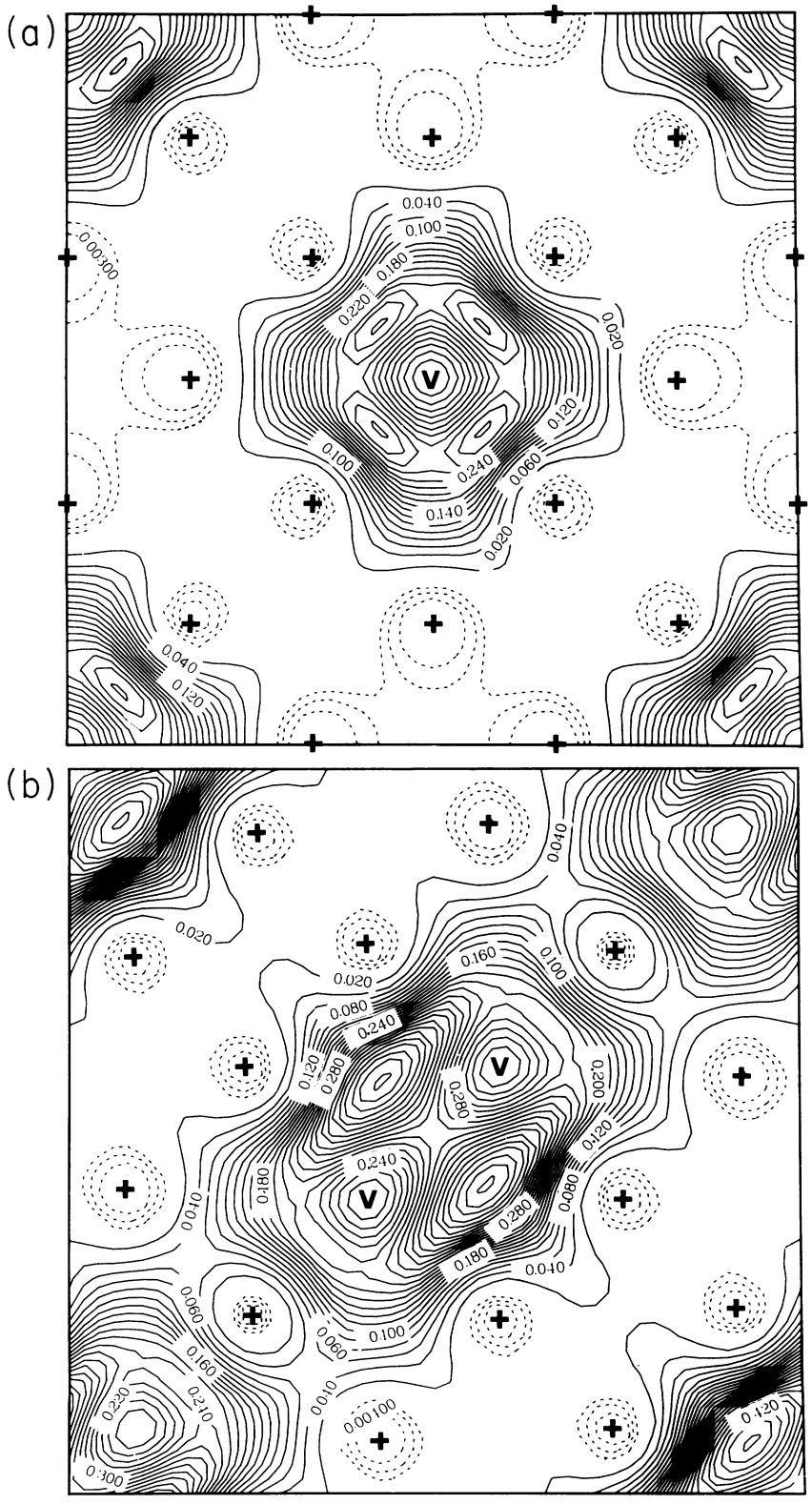

FIG. 8. Overlap of the function $\lambda(\vec{r})$ with the positron density (times the supercell volume) in the (100) plane around (a) a monovacancy (V) and (b) a divacancy (V-V). The atomic positions are denoted by $+$. The overlaps have been divided by the total number of electrons in the supercell.

TABLE IV. The positron lifetimes ($\tau \equiv \Lambda^{-1}$) in the monovacancy-trapped and divacancy-trapped states compared to other theoretical results and experiment (for the monovacancy). The valence (Λ_v) and core (Λ_c) contributions are also presented separately.

	Monovacancy				Divacancy			
	τ (ps)	Λ_v (ns^{-1})	Λ_c (ns^{-1})	Λ (ns^{-1})	τ (ps)	Λ_v (ns^{-1})	Λ_c (ns^{-1})	Λ (ns^{-1})
Present calculation								
(i) $a=4.0469$ Å	250	3.873	0.129	4.002	285	3.391	0.116	3.507
(ii) $a=4.1200$ Å	248	3.912	0.117	4.029				
(iii) $a=4.1323$ Å					279	3.486	0.103	3.589
Jellium calculation (Ref. 21)	237			4.22				
Nieminen and Puska (Ref. 30) ($a=4.0469$ Å)	253	3.87	0.081	3.95	273			3.66
McMullen *et al.* (Ref. 31) ($a=4.0412$ Å)	227[a]			4.40	255[b] 248[c]			3.92
APW calculation (Ref. 2) ($a=4.0483$ Å)	231	4.24	0.090	4.33				
Experiment (Ref. 17)	244							

[a]$\Lambda_c = 0.157\Lambda_v$ was assumed.
[b]Spherical divacancy.
[c]Elliptical divacancy.

the lifetime in a Brandt-Reinheimer formulation,[21] shows much less structure, but has the same overall magnitude.

The calculated positron lifetimes in the vacancy defects are shown in Table IV, and compared to other theoretical results and the experimental value for the positron lifetime in the monovacancy. In the theoretical calculations other than the present ones, the enhancement factors were estimated from the Brandt-Reinheimer formula for the valence electrons, while an average enhancement factor was used for the core electrons.[21] The core and valence contributions are shown separately in Table IV. It is seen that the lifetimes decrease with increasing lattice constant, which is consistent with a decreasing binding energy and, hence, with more leakage of the positron into the interstitial regions, where the electron density is high. Based on the lifetime information alone, it may be rather difficult to experimentally distinguish between a monovacancy and a divacancy. For actual defect spectroscopy, leading to a quantitative separation of the signals from the constituent defects in a vacancy ensemble, angular correlation spectra have to be examined. Experimentally, either one-dimensional or two-dimensional angular correlation spectra can be obtained. In the former, $R(\vec{p})$ has been integrated over two momentum components and contains much less information per spectrum than the two-dimensional spectra, which correspond to $R(\vec{p})$ integrated over one momentum direction. The present calculational scheme has been used to compute one- and two-dimensional angular correlation spectra, and the results have been used in conjunction with experiment to examine the presence of divacancies in aluminum.[28,29]

In the present work we would like to examine what type of electronic structure information regarding the defects in which positrons trap might be extracted from such experimental observations. The

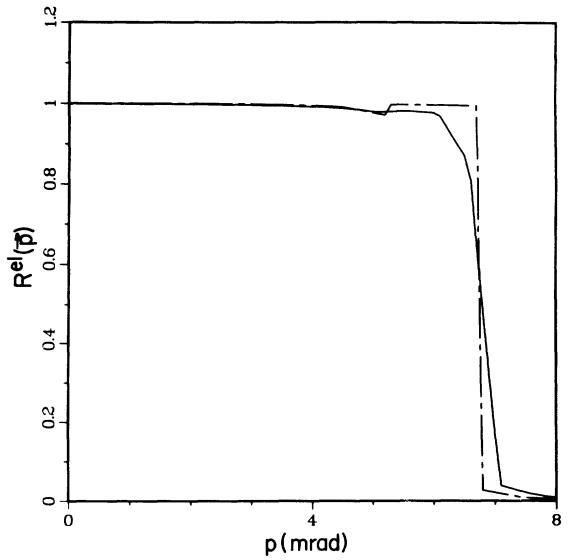

FIG. 9. Electron-momentum distribution function $R^{el}(\vec{p})$ along a ⟨100⟩ direction for a perfect lattice (dashed line) and a superlattice containing monovacancies (solid line).

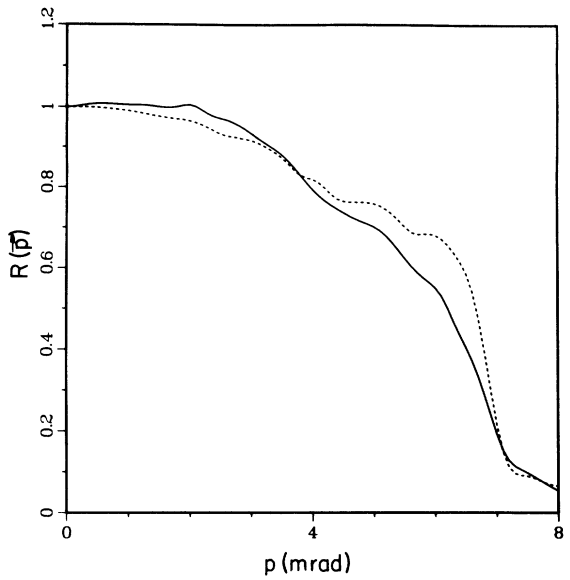

FIG. 10. Distribution function $R(\vec{p})$ along a $\langle 100 \rangle$ direction for the monovacancy-trapped positron state. The solid line is the result obtained with the actual form of $N(\epsilon)$ and the dashed line that obtained by substituting the Fermi distribution function for $N(\epsilon)$.

function $R(\vec{p})$ is like a momentum space density of states. When the positron is localized in defects, it can be seen from Eq. (5) that $R(\vec{p})$ gives local electronic structure information. However, if the positron could exist in a delocalized state in the presence of defects, $R(\vec{p})$ would give global information about the change in the host electron states caused by the defect, which is not expected to be a large effect. The function $R^{el}(\vec{p})$ for a perfect lattice and a superlattice containing monovacancies is shown in Fig. 9. This function was obtained from Eq. (6) by taking $N(\epsilon)$ to be the Fermi distribution function and the positron wave function to be a constant. The differences are seen to be small, the dominant effect being a broadening at the Fermi edge. The function $R(\vec{p})$ would yield local electronic structure information directly, if $N(\epsilon)$ were the Fermi distribution function and if $\psi^+(\vec{r})$ did not have too much structure. The second condition is close to the real situation, as can be seen from Fig. 6. To demonstrate the effect of $N(\epsilon)$, two plots are shown in Fig. 10, one of $R(\vec{p})$ with $N(\epsilon)$ replaced by the Fermi distribution function and the other of the actual $R(\vec{p})$. The functions in Fig. 10 show some noise, arising from not having enough $\vec{G}$ components of $A_{\vec{k}n}(\vec{G})$ in evaluating $R(\vec{p})$. It can nevertheless be seen from this figure that qualitative information can be obtained from $R(\vec{p})$, but to obtain quantitative information from experimental observations some means of deconvoluting $N(\epsilon)$ would have to be found. Interpretation of experimental information with regard to the detailed electronic structure of defects will, therefore, have to rely on accurate theoretical information about the positron-annihilation characteristics in a given defect configuration.

Before such calculations can be used to extract such quantitative detail from experiment, however, it will be necessary to address the question of structural relaxations around a defect in the presence of a trapped positron.[33] These can, in principle, be handled by the present scheme. The forces on the surrounding atoms can be calculated from the Hellmann-Feynman theorem, once the self-consistent electron and positron densities are known.[3] The next step would be to move the atoms along the direction of the total force, recalculate the forces, and repeat the process until equilibrium is reached. However, the uncertainties in the calculated forces make it hard to obtain an accurate quantitative result for the relaxed positions. Long-range relaxations cannot be handled in a supercell of the present size (cf. Sec. II B). However, a qualitative understanding can be obtained if the relaxations are small. The forces on the nearest-neighbor atoms around a monovacancy containing a trapped positron have been estimated in the present work and were found to be directed radially outward, indicating that an outward relaxation of these atoms would occur. Because of the previously mentioned uncertainties associated with such a calculation, however, the magnitude of these forces is not considered reliable and the calculation was not carried further. An efficient method for calculating relaxations would make the present calculational scheme even more valuable. One approach worth investigating is a parametrization of the forces in terms of the atomic positions followed by an analytic minimization. Such a scheme is being looked into at present.

V. CONCLUSION

The theoretical method presented here for calculating positron-annihilation characteristics is of general applicability. It can be used with any calculational scheme for studying defects, surfaces, or perfect solids. There are two drawbacks to this scheme; one is that it entails lengthy numerical calculations and the other is its inability to handle structural relaxations efficiently. A simpler scheme would be much more desirable. Nieminen and Puska[30] have developed such a scheme, but it suffers from the inability to incorporate electron-positron self-consistency. But, as is mentioned in Ref. 30, the positron lifetime is not very sensitive to self-consistency effects and can be calculated reliably.

However, if more detailed information regarding defects is desired, there seems to be no present alternative to lengthy calculations, such as those presented here.

ACKNOWLEDGMENTS

We would like to thank W. E. Pickett for calculating the nonlocal ionic pseudopotential and for many useful discussions. We would also like to thank D. Koelling for his Dirac-Slater atomic structure code, used here to calculate the electron core wave functions and the aluminum ionic potential. This work was supported by the U.S. Department of Energy.

APPENDIX: TWO-COMPONENT DENSITY-FUNCTIONAL FORMALISM

A derivation of the self-consistent set of equations [Eq. (2)] from a two-component density-functional scheme is presented in this section. The formulation of the density-functional scheme is closely analogous to spin-density-functional theory.[22] We consider a system of N particles, electrons plus positrons, and indicate the electron and positron densities by $n^-(\vec{r})$ and $n^+(\vec{r})$, respectively. The Hamiltonian for the system is

$$\hat{H}=\hat{T}+\sum_i V^{\sigma_i}(\vec{r}_i)+\hat{V}_e\ ,$$
$$\hat{V}_e=\tfrac{1}{2}\sum_{i,j}\frac{\sigma_i\sigma_j}{|\vec{r}_i-\vec{r}_j|}\ . \tag{A1}$$

In this equation σ is plus for a positron and minus for an electron, so σ_i depends on whether an electron or a positron occupies the position $\vec{r}_i$. Here, $\hat{T}$ is the kinetic energy operator, $\hat{V}_e$ is the Coulomb interaction, and $V^\sigma(\vec{r})$ is the external potential felt by the electron ($\sigma=-$) or positron ($\sigma=+$). This potential would be a simple function of σ for ionic potentials, $V^\sigma(\vec{r})=\sigma V_{\rm ion}(\vec{r})$. For pseudopotentials, however, this relation does not hold. A universal function $Q[n^-,n^+]$ is defined as

$$Q[n^-,n^+]=\min\langle\hat{T}+\hat{V}_e\rangle\ . \tag{A2}$$

The set of all N-particle antisymmetric functions producing the electron and positron densities $n^\sigma(\vec{r})$ is searched to obtain the minimum expectation value represented by $Q[n^-,n^+]$. The variational principle $\langle\hat{H}\rangle\geq E$, where E is the ground-state energy, then implies that for any choice of the trial densities $n^\sigma(\vec{r})$ representing N particles,

$$Q[n^-,n^+]+\int d\vec{r}\sum_\sigma V^\sigma(\vec{r})n^\sigma(\vec{r})\geq E\ . \tag{A3}$$

The true ground-state densities are those that make Eq. (A3) an equality. This is a generalized Hohenberg-Kohn[34] theorem. If the functional dependence of $Q[n^-,n^+]$ on $n^-(\vec{r})$ and $n^+(\vec{r})$ were known, Eq. (A3) could be used to calculate $n^-(\vec{r})$ and $n^+(\vec{r})$. For this purpose, it is convenient to break up $Q[n^-,n^+]$ into three parts:

$$Q[n^-,n^+]=T[n^-,n^+]+U[n^-,n^+]+E_{\rm xc}[n^-,n^+]\ , \tag{A4}$$

where $T[n^-,n^+]$ is the noninteracting kinetic energy, $U[n^-,n^+]$ is the direct Coulomb energy, and $E_{\rm xc}[n^-,n^+]$ is the exchange-correlation energy. Next, we write the electron and positron densities in terms of orthonormal orbitals $\psi_\alpha^\sigma(\vec{r})$ and occupation numbers f_α^σ,

$$n^\sigma(\vec{r})=\sum_\alpha f_\alpha^\sigma|\psi_\alpha^\sigma(\vec{r})|^2\ . \tag{A5}$$

The kinetic energy is defined as[22]

$$T[n^-,n^+]=\min\left[\sum_{\alpha,\sigma}f_\alpha^\sigma\langle\psi_\alpha^\sigma|(-\tfrac{1}{2}\nabla^2)|\psi_\alpha^\sigma\rangle\right]\ . \tag{A6}$$

The next step is to minimize

$$\tilde{E}=T[n^-,n^+]+U[n^-,n^+]+E_{\rm xc}[n^-,n^+]+\int d\vec{r}\sum_\sigma V^\sigma(\vec{r})n^\sigma(\vec{r}) \tag{A7}$$

with respect to the orbitals $\psi_\alpha^\sigma(\vec{r})$, subject to the normalization constraint of the orbitals. The Euler equation for this is

$$\frac{\delta}{\delta\psi_\alpha^\sigma(\vec{r})}\left[\tilde{E}-\sum_{\alpha',\sigma'}\epsilon_{\alpha'}^{\sigma'}f_{\alpha'}^{\sigma'}\int d\vec{r}\,|\psi_{\alpha'}^{\sigma'}(\vec{r})|^2\right]=0\ , \tag{A8}$$

where ϵ_α^σ are Lagrange multipliers. This leads to a set of one-particle self-consistent equations,

$$[-\tfrac{1}{2}\nabla^2+V_{\rm eff}^\sigma(\vec{r})]\psi_\alpha^\sigma(\vec{r})=\epsilon_\alpha^\sigma\psi_\alpha^\sigma(\vec{r})\ ,$$
$$V_{\rm eff}^\sigma(\vec{r})=V^\sigma(\vec{r})+\tfrac{1}{2}\sigma\sum_{\sigma'}\sigma'\int\frac{d\vec{r}\,'n^{\sigma'}(\vec{r}\,')}{|\vec{r}-\vec{r}\,'|}+\frac{\delta}{\delta n^\sigma(\vec{r})}E_{\rm xc}[n^-,n^+]\ . \tag{A9}$$

At this stage, an approximation has to be made for $E_{\rm xc}[n^-,n^+]$, since the exact form is not known. In

the local-density approximation, E_{xc} can be written as

$$E_{xc}[n^-,n^+]=\sum_\sigma \int d\vec{r}\, n^\sigma(\vec{r}) \times \epsilon_{xc}^\sigma(n^-(\vec{r}),n^+(\vec{r}))\ , \tag{A10}$$

where $\epsilon_{xc}^\sigma(n^-(\vec{r}),n^+(\vec{r}))$ is the exchange-correlation energy per particle of a homogeneous system with densities $n^-(\vec{r})$ and $n^+(\vec{r})$. Thus

$$\epsilon_{xc}^\sigma(n^-(\vec{r}),n^+(\vec{r}))=\epsilon_x(n^\sigma(\vec{r}))+\epsilon_c(n^\sigma(\vec{r})) +\epsilon_{corr}(n^\sigma(\vec{r}),n^{\sigma'}(\vec{r}))\ , \tag{A11}$$

where $\sigma'\neq\sigma$ in the third term. The first term is the exchange term, the second is the correlation among particles of the same type, and the last term is the correlation energy among particles of opposite charge. The electron-gas calculations of ϵ_{xc} deal with a system of *one* positron in an electron gas of arbitrary density.[24,25] The electron-positron correlation energy in these calculations is obtained as the change in ground-state energy of the electron system when one positron is introduced, which includes the change in the direct Coulomb energy of the system. However, the electron-gas calculations give no information about $\epsilon_{corr}(n^-(\vec{r}),n^+(\vec{r}))$ for an arbitrary positron density. We therefore have to make a single-positron approximation and write the effective potentials as

$$V_{eff}^-(\vec{r})=V^-(\vec{r})+\tfrac{1}{2}\int d\vec{r}\,'\frac{n^-(\vec{r}\,')}{|\vec{r}-\vec{r}\,'|} +\frac{\partial}{\partial n^-(\vec{r})}n^-(\vec{r})[\epsilon_x(n^-(\vec{r}))+\epsilon_c(n^-(\vec{r}))]+n^+(\vec{r})\frac{\partial}{\partial n^-(\vec{r})}\epsilon_{corr}^{-+}(n^-(\vec{r}))\ , \tag{A12}$$

$$V_{eff}^+(\vec{r})=V^+(\vec{r})-\tfrac{1}{2}\int\frac{d\vec{r}\,'n^-(\vec{r}\,')}{|\vec{r}-\vec{r}\,'|}+\epsilon_{corr}^{-+}(n^-(\vec{r}))\ ,$$

where $\epsilon_{corr}^{-+}(n^-(\vec{r}))$ is the electron-positron correlation energy obtained from the electron-gas calculations for the single positron. The self-consistent equations presented in the text [Eq. (2)] can be obtained by substituting Eq. (A12) into Eq. (A9).

The set of pair-distribution functions $\langle d_0^\dagger d_0 c_i^\dagger c_j\rangle$ have to be evaluated in the interacting ground state in order to be able to calculate the momentum distribution of the electron-positron pair. In the noninteracting ground state, only the $i=j$ functions survive. These are still the dominant terms in the actual ground state, since higher-order processes, involving the excitation of an electron from a state j to a state i, give rise to the nondiagonal ($i\neq j$) terms. In the present work, only the diagonal distribution functions have therefore been retained.

With the use of Feynman's theorem, a diagonal distribution function can be written as

$$\langle d_0^\dagger d_0 c_i^\dagger c_i\rangle=\left.\frac{\delta E_i(\beta)}{\delta\beta}\right|_{\beta=0}\ . \tag{A13}$$

Here $E_i(\beta)$ is the ground-state energy of a modified Hamiltonian

$$\hat{H}_i(\beta)=\hat{H}+\beta d_0^\dagger d_0 c_i^\dagger c_i\ , \tag{A14}$$

where β is an arbitrary parameter. This type of procedure was used by Lam and Platzman to calculate Compton scattering profiles.[35] The β dependence of $E_i(\beta)$ arising from variations in $n^-(\vec{r})$ and $n^+(\vec{r})$ can be neglected to first order, because of the stationary property of the ground-state energy. The only other source of β dependence is the electron-positron interaction energy. Making both the single-positron and the local-density approximations, Eq. (A13) can be written as

$$\langle d_0^\dagger d_0 c_i^\dagger c_i\rangle=\int d\vec{r}\left[\left.\frac{\partial\epsilon_{corr}^{-+\beta}(n^-(\vec{r}))}{\partial\beta}\right|_{\beta=0}\right]n^+(\vec{r})\ . \tag{A15}$$

Here, $\epsilon_{corr}^{-+\beta}(n^-(\vec{r}))$ is the correlation energy in a homogeneous electron gas, where the Hamiltonian has undergone the transformation specified by Eq. (A14), and hence is implicitly dependent on i. In an electron gas, the states i are momentum eigenstates and the term within large parentheses in Eq. (A15) is the electron-positron pair momentum distribution function in an electron gas [cf. Eq. (5)]. Thus the distribution function in the homogeneous system can be written as

$$N(\epsilon_i)\equiv\langle d_0^\dagger d_0 c_i^\dagger c_i\rangle =\int d\vec{r}\,N^0(\epsilon_i,n^-(\vec{r}))n^+(\vec{r})\ , \tag{A16}$$

where $N^0(\epsilon,n^-(\vec{r}))$ denotes the electron-gas pair momentum distribution function, expressed as a function of the energy $\epsilon=p^2/2m$.

*Present address: NORDITA Blegdamsvej 17, DK-2100 Kobenhavn Ø, Denmark.

[1]S. G. Louie, M. Schlüter, J. R. Chelikowsky, and M. L. Cohen, Phys. Rev. B 13, 1654 (1976).

[2]R. P. Gupta and R. W. Siegel, Phys. Rev. Lett. 39, 1212 (1977); Phys. Rev. B 22, 4572 (1980).

[3]B. Chakraborty, R. W. Siegel, and W. E. Pickett, Phys. Rev. B 24, 5445 (1981).

[4]B. Chakraborty and R. W. Siegel, in *Proceedings of the Yamada Conference V on Point Defects and Defect Interactions in Metals, Kyoto, 1981,* edited by J. Takamura *et al.* (University of Tokyo Press, Tokyo, 1982), p. 93.

[5]G. A. Baraff and M. Schlüter, Phys. Rev. Lett. 41, 892 (1978); Phys. Rev. B 19, 4965 (1979).

[6]J. Bernholc, N. O. Lipari, and S. T. Pantelides, Phys. Rev. Lett. 41, 895 (1978); Phys. Rev. B 21, 3545 (1980).

[7]R. Zeller and P. H. Dederichs, Phys. Rev. Lett. 42, 1713 (1979); R. Podloucky, R. Zeller, and P. H. Dederichs, Phys. Rev. B 22, 5777 (1980).

[8]R. W. Siegel, in *Advanced Techniques for Characterizing Microstructures,* edited by F. W. Wiffen and J. A. Spitznagel (The Metallurgical Society of AIME, Warrendale, 1982), p. 413.

[9]R. W. Siegel, in *Proceedings of the Sixth International Conference on Positron Annihilation, Fort Worth, 1982,* edited by P. G. Coleman *et al.* (North-Holland, Amsterdam, 1982), p. 351.

[10]B. Chakraborty, Phys. Rev. B 24, 7423 (1981); in Proceedings of the Second National Symposium on Positron Annihilation, Madras, 1982, edited by V. Devanathan and K. P. Gopinathan (South Asian, New Delhi, in press); in *Proceedings of the Sixth International Conference on Positron Annihilation, Fort Worth, 1982,* edited by P. G. Coleman *et al.* (North-Holland, Amsterdam, 1982), p 207.

[11]R. Zeller, P. J. Braspenning, J. Deutz, R. Podloucky, and P. H. Dederichs, in *Proceedings of the Yamada Conference V on Point Defects and Defect Interactions in Metals, Kyoto, 1981,* edited by J. Takamura *et al.* (University of Tokyo Press, Tokyo, 1982), p. 97.

[12]D. R. Hamann, M. Schlüter, and C. Chiang, Phys. Rev. Lett. 43, 1494 (1979).

[13]P. K. Lam and M. L. Cohen, Phys. Rev. B 24, 4224 (1981).

[14]J. F. Janak, V. L. Moruzzi, and A. R. Williams, Phys. Rev. B 12, 1257 (1975).

[15]The lattice constant at 0 K was obtained by a linear extrapolation to $\Theta_D/3=131$ K of the room-temperature results: (a) K. A. Gschneidner, Jr., in *Solid State Physics,* edited by H. Ehrenreich, F. Seitz, and D. Turnbull (Academic, New York, 1964), Vol. 16, p. 276 and (b) *American Institute of Physics Handbook,* 3rd ed., edited by D. E. Grey (McGraw-Hill, New York, 1972); see Table 9a-2. This was taken to be the value of a at 0 K. The temperature coefficient was obtained from N. W. Ashcroft and N. D. Mermin, *Solid State Physics* (Holt, Rinehart and Winston, New York, 1976), p. 496. (c) *Physical Acoustics,* edited by W. P. Mason (Academic, New York, 1965), Vol. III B, p. 84, and Ref. 30 of Ref. 3.

[16]R. A. Coldwell-Horsefall and A. A. Maradudin, J. Math. Phys. 1, 395 (1960).

[17]M. J. Fluss, L. C. Smedskjaer, M. K. Chason, D. G. Legnini, and R. W. Siegel, Phys. Rev. B 17, 3444 (1978).

[18]A. S. Berger, S. T. Ockers, and R. W. Siegel, J. Nucl. Mater. 69-70, 734 (1978).

[19]S. G. Louie, K. M. Ho, and M. L. Cohen, Phys. Rev. B 19, 1774 (1979).

[20]R. Benedek (private communication); M. C. Lega and S. C. Ying, Solid State Commun. 40, 37 (1981).

[21]R. M. Nieminen and M. J. Manninen, in *Positrons in Solids,* edited by P. Hautojärvi (Springer, Berlin, 1981), p. 145.

[22]J. P. Perdew and A. Zunger, Phys. Rev. B 23, 5048 (1981).

[23]P. Kubica and M. J. Stott, J. Phys. F 4, 1969 (1974).

[24]J. Arponen and E. Pajanne, Ann. Phys. (N.Y.) 121, 343 (1979); J. Phys. C 12, L161 (1979).

[25]D. Neilson, in *Proceedings of the Sixth International Conference on Positron Annihilation, Fort Worth, 1982,* edited by P. G. Coleman *et al.* (North-Holland, Amsterdam, 1982), p. 192.

[26]E. Bonderup, J. U. Andersen, and D. N. Lowy, Phys. Rev. B 20, 883 (1979).

[27]J. A. Appelbaum and D. R. Hamann, Phys. Rev. B 8, 1777 (1973).

[28]M. J. Fluss, S. Berko, B. Chakraborty, K. Hoffmann, P. Lippel, and R. W. Siegel (unpublished).

[29]B. Chakraborty, S. Berko, M. J. Fluss, K. Hoffmann, P. Lippel, and R. W. Siegel, in Proceedings of the Second National Symposium on Positron Annihilation, Madras, 1982, Ref. 10; M. J. Fluss, S. Berko, B. Chakraborty, K. Hoffman, P. Lippel, and R. W. Siegel, in *Proceedings of the Sixth International Conference on Positron Annihilation, Forth Worth, 1982,* Ref. 10, p. 454.

[30]M. J. Puska and R. M. Nieminen, J. Phys. F 13, 333 (1983).

[31]T. McMullen, R. J. Douglas, N. Etherington, B. T. A. McKee, A. T. Stewart, and A. Zaremba, J. Phys. F 11, 1435 (1981).

[32]G. Lehmann and M. Taut, Phys. Status Solidi 54, 469 (1972).

[33]S. W. Tam and R. W. Siegel, J. Phys. F 7, 877 (1977).

[34]P. Hohenberg and W. Kohn, Phys. Rev. 136, B864 (1964).

[35]L. Lam and P. M. Platzman, Phys. Rev. B 9, 5122 (1974).